Clinical-grade production and safe delivery of human ESC derived RPE sheets in primates and rodents

Karim Ben M'Barek, Stephane Bertin, Elena Brazhnikova, Céline Jaillard,
Walter Habeler, Alexandra Plancheron, Claire-Maëlle Fovet, Joanna Demilly,
Mohamed Jarraya, Ana Bejanariu, et al.

Title page

Clinical-grade production and safe delivery of human ESC derived RPE sheets in primates and rodents

Karim Ben M'Barek[1,2,3], Stéphane Bertin[4], Elena Brazhnikova[5], Céline Jaillard[5], Walter Habeler[1,2,3], Alexandra Plancheron[1,2,3], Claire-Maëlle Fovet[6], Joanna Demilly[6], Mohamed Jarraya[7], Ana Bejanariu[3], José-Alain Sahel[4,5,8], Marc Peschanski[1,2,3], Olivier Goureau[5*] and Christelle Monville[1,2*]

[1]INSERM U861, I-Stem, AFM, Institute for Stem cell Therapy and Exploration of Monogenic diseases, 91100 Corbeil-Essonnes, France;

[2]UEVE U861, I-Stem, AFM, Institute for Stem cell Therapy and Exploration of Monogenic diseases, 91100 Corbeil-Essonnes, France;

[3]CECS, I-Stem, AFM, Institute for Stem cell Therapy and Exploration of Monogenic diseases, 91100 Corbeil-Essonnes, France;

[4]CHNO des Quinze-Vingts, DHU Sight Restore, INSERM-DGOS CIC 1423, Paris, France

[5]Institut de la Vision, Sorbonne Université, INSERM, CNRS, F-75012 Paris, France

[6]CEA-MIRCen, 92260 FAR, France

[7]Banque de tissus humain, Hôpital Saint Louis, Assistance Publique - Hôpitaux de Paris (AP-HP), Paris, France

[8]Department of Ophthalmology, University of Pittsburgh School of Medicine, Pittsburgh, PA 15213, USA.

* These authors contributed equally to this work.

Correspondence should be addressed to: cmonville@istem.fr and olivier.goureau@inserm.fr

Abstract (200 words)

Age-related macular degeneration as well as some forms of Retinitis Pigmentosa (RP) are characterized by a retinal degeneration involving the retinal pigment epithelium (RPE). Various strategies were proposed to cure these disorders including the replacement of RPE cells using human pluripotent stem cells (hPSCs), an unlimited source material to generate *in vitro* RPE cells. The formulation strategy of the cell therapy (either a reconstructed sheet or a cell suspension) is crucial to achieve an efficient and long lasting therapeutic effect. We previously developed a hPSC-RPE sheet disposed on human amniotic membrane that sustained the vision of rodents with retinal degeneration compared to the same cells injected as a suspension. However, the transplantation strategy was difficult to implement in large animals. Herein we developed two medical devices for the preparation, conservation and implantation of the hPSC-RPE sheet in nonhuman primates. The surgery was safe and well tolerated during the 7-week follow up. The graft integrity was preserved in primates. Moreover, the hPSC-RPE sheet did not induce teratoma or grafted cell dispersion to other organs in rodent models. This work clears the way for the first cell therapy for RP patients carrying RPE gene mutations (*LRAT*, *RPE65* and *MERTK*).

25 words brief summary:

Specifically developed medical devices ensure the preparation and delivery of bio-engineered hESC-RPE sheets into rodent and nonhuman primate eyes, without safety issues.

Keywords: cell therapy, human pluripotent stem cells, Retinitis Pigmentosa, age-related macular degeneration.

Introduction

The retinal pigment epithelium (RPE), a supportive tissue for photoreceptor (PR) homeostasis and survival, could be affected in various disease conditions including some forms of Retinitis Pigmentosa (RP) and age-related macular degeneration (AMD) (1). The dysfunction or death of RPE cells triggers the secondary death of PRs and ultimately leads to vision loss. RP is a group of inherited disorders with more than 80 genes identified, which could affect specifically RPE cells, PRs or both (2-4). The mutations leading to RPE cell dysfunctions account for 5% of all RP patients (3, 5). There is no cure for RP, despite the recent approval of a gene therapy that could only target a minority of patients carrying a mutation in the *RPE65* gene (6). AMD is a complex disease caused by the combination of genetic and environmental factors (7-10). This disease could evolve to a dry form or geographic atrophy with the death of RPE cells or to a wet form characterized by a choroidal neovascularization (CNV)(8, 11). The CNV could alter the RPE and its basement membrane (the Bruch's membrane)(8, 11). Therapeutic options are available to treat the wet form, such as the delivery of anti-angiogenic agents, while there is no treatment for the dry form which account for 80-90% of patients (5, 12). Stem cell-based therapy using RPE derived from human pluripotent stem cells (hPSCs) is one of the most promising strategies with a number of preliminary safety reports from clinical trials already published (13-18).

The strategy for the preparation and eye delivery of the cell therapy product, namely hPSC-derived RPE, is crucial for both the survival of the graft and its functionality (5, 19, 20). The cell survival was significantly improved in Nude rats when RPE cells were grafted as a sheet compared to a cell suspension (21). In addition, we have demonstrated that a sheet of RPE derived from human embryonic stem cells (hESCs) improved significantly photoreceptor preservation and consequently the visual restoration of rats with a retinal degeneration caused by a RPE defect, when compared to the same cells injected as a cell suspension (22). This hESC-RPE sheet was grown on a biological scaffold, the amniotic membrane,

3

which is relatively difficult to manipulate and requires a complex preparation process prior to transplantation. This preliminary preparation restricts its implementation in clinical trials. However, this biological scaffold contains a basement membrane more close to the one of endogenous RPE cells and therefore is attractive compared to already developed synthetic polymers (13, 16, 23). In addition, amniotic membranes are widely used in clinical practices with banking strategies that make it ready to use (24). Besides, these membranes hold other characteristics like a low immunogenicity, anti-inflammatory and anti-microbial properties (24-26).

Herein, we developed an original approach to prepare and store the hESC-RPE sheet (grown on amniotic membranes) as well as tools to implant the graft into the subretinal space of larger animals. For this purpose, two different medical devices were designed and validated for use in clinics. We then evaluated the feasibility and safety of the tissue-engineered product following transplantation in nonhuman primates. We also ruled out risks of teratoma formation and cell dispersion to other organs in Nude rodents. This preclinical development clears the way for a phase I/II clinical trial targeting RP patients with mutations affecting RPE cells.

Results

Embedding hESC-RPE sheets into gelatin using a dedicated Medical device

The hESC-RPE sheet has previously been described and characterized for its *in vitro* functionality and its ability to rescue the visual phenotype of the royal college of surgeons (RCS) rat model of RP (22, 27). Aiming at delivering the hESC-RPE sheet into the subretinal space of rats, we previously developed a strategy based on a gelatin embedding at 4°C for a few hours before the surgery. The gelatin-layer thickness was then adjusted using vibratome equipment (22, 27). This strategy allowed us to protect the hESC-RPE cells during implantation and provides elasticity and rigidity to the patch, which is rolled into the injector during the implantation procedure. Implementing this strategy in a clinical setting appears difficult due to the number of steps required and the variability that could be associated with these manipulations. To overcome these challenges, we simplified the production process of the hESC-RPE sheet by designing a medical device (MD1) allowing the addition of the gelatin layers without the use of a vibratome (**Figure 1A**). The hESC-RPE sheet was fixed on an insert during the four weeks of cell culture prior to gelatin embedding and controlled for its identity (RPE markers detection), purity (residual undifferentiated cells), potency (functional release of trophic factor), sterility and viability (**supplemental Figure S1**). The MD1 is composed of a central body (**Figure 1B**) containing a well allowing the positioning of a cell culture insert. A space of 150 µm is created between the hESC-RPE sheet and the surface of the device, by making a notch at the borders of the well, where the culture insert is placed (**Figure 1A**). A first cap (cap 1) is disposed on top of the central body of the device (**Figure 1C, 1D**) that creates another space of 150 µm on top of the hESC-RPE sheet (**Figure 1A, 1D, supplemental Movie 1**). A warmed gelatin solution could be delivered on both sides thanks to holes that are included into the cap 1 and the central body of the device using a simple culture pipette (**Figure 1E, 1F, supplemental Figure S2**). Once the gelatin becomes rigid at 4°C, a transport culture medium is added inside the well of the body and the

5

container is closed with another cap (cap 2) to prevent fluid leakage. The system is stored at 4°C until use, in order to maintain gelatin rigidity.

hESC-RPE sheets embedded into gelatin are viable and functional for 48 hours at 4°C

We then evaluated both cell density and viability of the hESC-RPE sheet included in gelatin in order to test the stability of the sheet in the medical device MD1 (stored at 4°C). The cell density remained stable up to 48 hours, but decreased significantly at 72 hours compared to the time point before gelatin embedding (ANOVA $F_{(4,19)}=5.408$; **p=0.0044) (**Figure 2A, 2B**). The cell viability remained stable for all the time points (ANOVA $F_{(4,19)}=1.662$; p=0.2002) with a more variable cell viability at 72 hours (**Figure 2C**). We thus measured further the functionality of the hESC-RPE sheet embedded in gelatin within this 48 hour-period at 4°C. Cell potency was assessed, up to 48 hours at 4°C, through the quantification of the amount of VEGF released in the medium following subsequent culture. The amount of VEGF released in the medium did not change significantly before gelatin embedding (2008.5 pg/ml +/-188.5) and after 48h at 4°C with gelatin into MD1 (1804.6 pg/ml +/-796.9; Mann Whitney test: U=4; p=0.9). This 48-hour stability period was sufficient for the production of hESC-RPE sheets in gelatin at the good manufacturing practice (GMP) site and the transfer at 4°C by car to the distant site of nonhuman primate transplantation (374 km).

Method for hESC-RPE sheet sizing and implantation in enucleated pig eye

To facilitate the final size adjustment of the hESC-RPE sheet before final transplantation, we developed another medical device (MD2) composed of a punch and a cap (cap 3) that could be adapted to the first device (**Figure 3A, supplemental Movie 2**). The cap 3 was designed to guide the punch in order to cut the hESC-RPE sheet in a reproducible manner at the same position (**Figure 3B, supplemental Figure S3**). The punch is composed of a metal blade shaping a 14.5 mm^2 sim-card (**Figure 3C-D**). This shape ensures the assessment of the right hESC-RPE sheet polarity below the retina following transplantation. Once the

sheet is cut with the punch, it is loaded and rolled into a lens injector as previously described for injection (22). The rolled sheet is pushed into a longer injection cannula in order to transplant into large eyes (**Figure 3E-F, supplemental Movie 3**). To validate the different medical devices used to manufacture and manipulate the hESC-RPE sheet as well as the modified injection strategy, the graft was first implanted in enucleated pig eyes (**Figure 3G-J**). A saline solution is introduced under the retina to create a retinal detachment, followed by a retinotomy. Then the injector is introduced in the subretinal space to deliver the hESC-RPE sheet (**Figure 3J**). Once injected, the transplant colored with a blue dye became planar under the retina (**Figure 3K**) and the sim-card shape ensured the monitoring of correct transplant orientation with hESC-RPE cells contacting photoreceptors.

hESC-RPE sheets grafted in nonhuman primates keep their initial position during the experimental period (OCT)

The surgical strategy as well as the tolerance of the hESC-RPE sheet were performed in immunosuppressed nonhuman primates, which were implanted in one eye through a 3-port pars plana vitrectomy with cold vitreous cavity irrigation. The major steps of the surgery were the same as for enucleated pig eyes with the creation of a retinal detachment followed by a retinotomy and the graft injection (**supplemental Movie 4**). The hESC-RPE sheet was correctly implanted at the target location (macular area) without any major surgical complications such as significant retinal or choroidal bleeding, unplanned iatrogenic retinal detachment or retinal tears (**Figure 4A-B**). Once implanted, the position of the patch remained stable during the 7-week follow-up without signs of degradation, as visualized by ocular fundus microscopy and optical coherence tomography (**Figure 4A-C**), demonstrating that our transplantation tool safely delivered the patch.

Transitory inflammatory response without alteration of the retinal function following implantation in nonhuman primates

One-day post-surgery, a moderate inflammatory reaction of the anterior segment was observed by slit-lamp biomicroscopy in the treated eye of all animals (**Figure 5A-C**). Evaluation at two weeks demonstrated that inflammation was resolved in all transplanted animals, excepted in one monkey, where a marked level of vitreous opacification (vitreous haze) was noted during the first three weeks (**supplemental Figure S4**). This transitory inflammation might be caused by the surgical procedure rather than by the presence of hESC-RPE sheet in the subretinal space. The functionality of transplanted eyes was evaluated by electroretinography comparing eyes before implantation (baseline) to same eyes after implantation (post-surgery). Photopic electroretinography indicated that a-waves and b-waves were not significantly altered at 6 weeks post-surgery (**Figure 5D-E**). In addition, multifocal electroretinography performed at the level of hESC-RPE sheet location or outside the grafting area (non-detached area) showed that P1 amplitudes and implicit times remained comparable to the baseline (**Figure 5F-G**). This suggests that the functionality of the retina evaluated by electroretinography was not affected by the transplant.

hESC-RPE sheets grafted in nonhuman primates survive in close contact with photoreceptors and are functional.

We then evaluated the survival and integration of the hESC-RPE sheet, by immunofluorescence, in histological sections. Grafted cells, detected using the human specific STEM121 antibody, covered uniformly the human amniotic membrane, identified by Collagen IV staining, in the subretinal space (**Figure 6A-B**). Immunostaining with MERTK and Ezrin RPE markers confirmed their expression at the apical side of the hESC-RPE cells (**Figure 6A, 6D-E**), demonstrating that the hESC-RPE layer of the graft remained well polarized at 7-week post-transplantation. Importantly, the hESC-RPE sheet identified either by Ezrin or STEM121 staining was in contact with outer segments (OS) of photoreceptors, labeled with different antibodies against Recoverin (rods and cones), Red/Green opsin (red/green cones) , Blue

opsin (blue cones) and Rhodopsin (rods) (**Figure 6B-G**). The presence of Recoverin or Red /Green opsin staining in STEM121-positive or Ezrin-positive human cells indicates the ability of transplanted hESC-RPE cells to phagocytose photoreceptor OS (**Figure 6C-E**). Interestingly, Recoverin and R/G opsin staining (**Figure 6C** and **6D**) showed a slight reduction in OS length/size in the patch area compared to the area outside the patch. Taken together, these results indicate that the hESC-RPE sheet correctly faced the primate photoreceptors.

The immunosuppression of nonhuman primates was suboptimal during the course of the study. Despite regular adjustments for the majority of animals, the targeted range (cyclosporine blood levels between 250 to 400 ng/ml) was difficult to maintain during the course of the study (**supplemental Figure S5**). Indeed, only the primate 3 had a constant immunosuppression with cyclosporine blood levels precisely within the target values (from the day of the surgery to end of the follow up). However, the hESC-RPE sheets remained viable in all primates except in one case, where the epithelial layer contained less human cells and for which the blood level of cyclosporine was below the expected range of efficacy.

hESC-RPE cells or sheets are safe in rodent eyes

Two main safety concerns are associated with cell therapies based on the use of hPSC derivatives: teratoma formation due to residual contaminating stem cells and migration of cells out of the grafting site. To address the risk of teratoma formation that consists of benign tumors of normal karyotype containing cells derived from the three germ layers, a good laboratory practice (GLP) study was conducted. Since the subretinal space, which corresponds to the targeted site in humans, is less permissive to teratoma formation compared to the subcutaneous route (28, 29), hESC-RPE cells or hESCs were injected subcutaneously, corresponding to the worst-case scenario (escape of hESC-RPE cells from the eye). Nude mice (n=13) were injected with 1.10^6 hESC-RPE cells or with 1.10^6 hESCs (n=10) and followed up for 6 months. A histopathological evaluation was then conducted at the end of the study.

The control hESC treatment engendered teratomas containing two or three germ layers in 50% of cases (**Figure 7A-B**). By contrast, the injected hESC-RPE cells remained as a dark pigmented cluster of cells (11 out of 13 mice), without teratoma formation or associated mortality/toxicity until the end of the study (**Figure 7A**). There were also no metastasized cells in the other analyzed organs.

To address the second risk of hPSC-based therapy, we conducted a GLP study to evaluate the biodistribution and acute and chronic toxicity of the hESC-RPE sheet. Nude rats were implanted in the subretinal space with a hESC-RPE cell suspension, a hESC-RPE sheet or a control saline solution and animals were sacrificed at week 2 and 13 and at a last time point at week 26 only for the hESC-RPE sheet group. The presence of human cells was detected by qPCR for the presence of human specific *ALU* sequences in rat treated eye and organ extracts. As expected, no human cells were detected in animals injected with a saline solution (**supplemental Table S1**). Animals transplanted with the hESC-RPE sheet contained human cells only in the treated eye at all analyzed time points (**supplemental Table S2**). When a suspension of hESC-RPE cells was delivered into Nude rats, the human cells were only detected into the treated eye and associated optic nerves, but not in other organs (**supplemental Table S3**). It indicates that human cells from hESC-RPE sheets or in cell suspension do not migrate at distance from the injection site in all analyzed time points. Interestingly, cell suspension persistence is significantly reduced compared to hESC-RPE sheets as indicated by the lower number of treated eyes where human cells could be detected (**Figure 7C**). No signs of toxicity were associated with any of these treatments (mortality, histopathology). Taken together, these data support the safety of the hESC-RPE sheet as transplanted cells do not induce teratomas or migrate outside of the grafting site and are not toxic in rodents.

Discussion

In this study, we developed a simplified method to produce and store a hESC-RPE sheet suitable for transplantation using two separate medical devices. This hESC-RPE sheet could be safely delivered in the eye of nonhuman primates without adverse events or functional alterations. In addition, this hESC-RPE sheet neither induced teratoma nor biodistribution issues in Nude rodents. The grafted cells also survived without phenotypic alterations in the eye of nonhuman primates and rodents during the follow up period.

The formulation strategy of the RPE cell therapy has dramatic consequences on both survival and functionality. Indeed, early studies were conducted using cell suspensions in rodent and have demonstrated the functionality of such strategy (30-33). However, the sheet formulation improved the survival in the subretinal space and increased the functionality compared to simple cell suspensions (21, 22). Herein the biodistribution study conducted in Nude rats confirmed previous results regarding the lower survival potential of RPE cells injected as a cell suspension. Indeed, the endogenous RPE layer in rat models is still present and may limit the correct integration of isolated grafted RPE cells. Regarding AMD patients, the Bruch's membrane in which endogenous RPE cells adhere may also be damaged as in the case of a wet form (34). In addition, a diseased eye environment could also affect the potency of isolated RPE cells to assemble as a tight epithelium. A limited epithelial reformation may have dramatic consequences regarding functionality (19, 35-37). Thus, despite the easy implementation of such cell suspension formulation in clinic, efforts are directed now to formulate RPE cell therapies with an organized sheet as the one described in this study (38). First clinical trials have demonstrated the safety of the hPSC-RPE cell therapy (as cell suspension or as a sheet) with some early signs of efficacy reported (13, 15-17). However, It is very difficult to compare the effectiveness between the two types of approaches as the cohort size is limited in these clinical trials, patients are legally blind or with low vision, and are not necessarily affected by the same disease.

Different strategies were proposed to generate RPE sheets including the use or not of scaffolds to reconstruct the RPE epithelium *in vitro* (19, 38, 39). The group of M. Takahashi developed a RPE sheet without scaffold by growing the RPE cells in a collagen matrix and used a collagenase to detach the sheet (17, 30). However, the RPE sheet remains complex to manipulate and needs particular handling skills to be correctly transplanted in patients. Other alternatives are based on scaffolds made of synthetic polymers. These scaffolds are rigid and easier to manipulate but specific injection systems are still required (13, 16, 23). We chose herein a biological scaffold that is closer to the RPE native environment, the human amniotic membrane. This scaffold contains a basement membrane and allows the formation of an epithelium without prior coating with proteins. Beside its role in RPE cell culture, the amniotic membrane by itself provides an additional transitory effect on photoreceptor survival when transplanted alone in RCS rats, increasing thus the interest on this specific scaffold (22). The complexity of the preparation was however difficult to implement for clinical trials (27). Therefore, we simplified the preparation of the hESC-RPE sheet at the manufacturing site and in the surgery facility by the development and validation of two medical devices. Moreover, we extended the stability of the hESC-RPE sheet from few hours to 48 hours, facilitating its storage and transport to the hospital without requirement of cell culture incubators. This method is susceptible to enhance the ability to deliver the cell therapy to multiple distant hospitals compared to current methods (13, 16, 17, 23).

The hESC-RPE sheet correctly facing and contacting primate photoreceptors and detection of events of OS phagocytosis by immunofluorescence suggest that hESC-RPE cells are functional. The slight reduction in OS length/size observed in the patch area could be due to the implantation method of the hESC-RPE sheet, or the space occupied by the hESC-RPE sheet (including amniotic membrane) and do not affect retinal function, at least during the 7-week study period. Future studies with longer follow up will determine if this phenomenon is transitory. Indeed, the absence of contact between RPE and photoreceptors, as observed in the case of electronic implants grafting between RPE and photoreceptors

in rats (40, 41) can lead photoreceptors to quickly degenerate. In our previous experiments in the Royal College of Surgeons rat presenting a specific defect in the phagocytosis function of endogenous RPE that engenders the accumulation of OS debris and photoreceptor cell death, we observed that the hESC-RPE sheet sustained the photoreceptor survival during the 3-month follow up which indicates that grafted cells were able to eliminate photoreceptor OS debris and prevent their death (22). This observation confirmed that true integration of the hESC-RPE sheet rather than a neurotrophic effect of the patch can prevent photoreceptor cell death.

The hESC-RPE sheet was demonstrated to be safe in Nude mice and rats in the two GLP studies, clearing thus the way for a clinical application. These results are in accordance with previous studies based on human PSC derived RPE conducted both in rodents and patients (13-17, 23). There is however a concern regarding the immune reaction due to the mismatch of the human leukocyte antigen (HLA) of hESC-RPE sheets and the patient. In this study, we administered an immunosuppressive treatment to the nonhuman primates and despite a suboptimal treatment in a xenograft context, the hESC-RPE sheet remained stable for the majority of cases. For the recent published clinical trials based on hPSCs, immunosuppression was ranged from systemic to local treatments (13-16). Results obtained with these different approaches may help future clinical trials to choose adapted strategy to prevent graft rejection, considering that systemic immunosuppression has major side effects in patients. As an alternative to such treatment, the HLA between hPSC-RPE cells and the recipient could be matched by generating hPSCs banks of known HLA (42-44). In this context, an estimation of 150 HLA-selected donors of hPSC lines should cover 93% of the UK population (45). A clinical trial is currently on going in Japan based on HLA-matched hPSC-RPE cells (5).

We developed a method to produce a hESC-RPE sheet on a biological scaffold that met all the regulatory requirements for a clinical use ranging from the GMP manufacturing (hESC-RPE banks and hESC-RPE sheet productions) to GLP *in vivo* safety studies. This cell therapy has reached regulatory agreements

from French health authorities for a phase I/II clinical trial to treat RP patients with RPE associated mutations (*LRAT*, *RPE65*, *MERTK*). As first RPE cell therapy for RP, results of this clinical trial will demonstrate the first proof of concept in human and, if a preliminary efficacy is reported, will be supportive for an extension to AMD patients.

Methods

Animal studies

Animal experimentations have been designed to respect the 3R (reduce, refine, replace) principle. Animal studies comply with the European Parliament Directive 2013/063. Nude mice and Nude rats studies were conducted also in accordance with the Directive 2004/10/EC for good laboratory practice (GLP) studies. Nonhuman Primate experiments were conducted after local CEA ethical committee (CETEA DSV n°44) and French Ministry of Agriculture study approval (agreement number for this study APAFIS# 10085-20170531 16318262 v3), in animal facilities licensed by the "direction départementale de la protection des populations" (agreement B92-032-02). All procedures regarding eye implantation and evaluation are in accordance with the ARVO statement for animal research in ophthalmology.

hESC-RPE culture and sheet preparation

Clinical grade hESCs line RC-09 derivation was previously described (22, 46). hESCs were maintained by daily media renewal with Stem Pro (Thermo Fisher Scientific) supplemented with FGF2 (10ng/ml) and manually passaged each week as small clumps. The hESC-RPE cells were obtained by spontaneous differentiation in a differentiation medium containing 20% Knock-out serum replacement (KSR, Thermo Fisher Scientific) as previously described (22). Briefly, after 6-8 weeks pigmented patches were collected and seeded in new culture plates with a culture medium supplemented with 4% KSR as previously described (22). hESC-RPE cells were banked and qualified for sterility, stability, potency, identity, purity and stability following guidelines for human cell banks (22). hESC-RPE sheets are obtained by seeding on a decellularized human amniotic membrane fixed in a custom maid culture insert for 4 weeks. After this initial culture period, inserts are washed with PBS and placed dry in the sterile medical device MD1, closed with the cap 1. The 2 compartments are filled sequentially with a gelatin solution (Nitta gelatin, diluted in a saline solution) on both sides and placed at 4°C few minutes for polymerization. Once polymerized, the cap 1 is removed and the MD1 is filled with a conservation medium (Stem Alpha1) and

closed with the cap 2. The MD1 is stored at 4°C (+/- 3) up to 48 hours until use. At the surgery site, the MD1 is opened and washed twice with BSS (Alcon) and colored with an ophthalmic blue dye (Membrane Blue Dual, DORC). The MD2 is used to cut the hESC-RPE sheet at the desired size ($14.5mm^2$) and shape. The sheet is then placed in a first injection system to fold the graft (Viscoject, Medicel) and then transferred to a 16 Ga cannula (BD Insyte Autoguard, BD Vialon Material). The cannula is beveled to identify the position of the hESC-RPE layer. A cannula of a smaller diameter (18Ga) is placed inside the first one in order to push the graft when on the subretinal space. Both cannulas are placed in cold BSS until implantation.

Primate transplantation

Nonhuman Primates were anesthetized by an intramuscular injection of ketamine (10 mg/kg) and xylazine (5 mg/kg) and maintained with an intravenous infusion of Propofol 1ml/kg/hour, followed by a local ocular anesthesia (oxybuprocaine chlorhydrate, Thea). Pupillary dilatation was achieved with 0.5 % tropicamide eye drops (Mydriaticum) at least 20-25 minutes before intervention. The non-operated eye was protected with an ophthalmic gel (Lubrithal, Dechra) to prevent dehydration. Subretinal implantation of the hESC-RPE sheet was performed through a 3-port pars plana vitrectomy with cold vitreous cavity irrigation (BBS plus, Alcon at +4°C) under a stereomicroscope (Lumera 700, Zeiss). The vitrectomy (23 Ga ports) was realized using Alcon Constellation. A bleb for the retinal detachment was then created by subretinal injection of BSS with a subretinal cannula in the macular area. Prior to retinotomy, the appropriate area of the retina was coagulated. A retinotomy of 2mm was performed using microscissors. The scleral incision of 2mm was created to introduce the injection system via the pars plana into the vitreous cavity. The graft was then delivered through the retinotomy. After the hESC-RPE sheet delivery the sclerotomy was then closed. The retina was attached under PFCL (Perfluorocarbon liquid DECA, DORC). A laser photocoagulation (VITRA LASER, QUANTEL MEDICAL) was then applied to the area of the retinotomy. After a fluid/air followed by an air/ 20% SF6 gas (Physiol)

16

exchange, the trocars were removed and the additional portion of the 20% SF6 gas was added if needed. The conjunctive was closed with a 7-0 suture and the animal was allowed to awake progressively by intravenous propofol withdrawal.

Teratoma GLP study

Nude mice (SOPF - BALB/cOlaHsd-Fox1^{nu}) were purchased from Envigo and grafted at 6 to 8 weeks of age. Animals were housed by groups of 5, under an artificial day/light cycle of 12 hours and fed *ad libitum*. Males and females were treated with a hESC-RPE suspension (10^6 cells) diluted in matrigel (Corning) or hESCs (10^6 cells) through a subcutaneous route in the middle back between the front and back limbs. Mortality was recorded twice daily. Injection site was evaluated every 3 days by palpation to follow the cell mass. An ethical size limit of the tumor was fixed at 1cm^3. Animals that exceeded this limit were sacrificed before the end of the study (2 anticipatory sacrifices in the hESCs group). Animals were followed up until week 26 and then sacrificed after an overnight fasting. The necropsy was conducted by an anatomopathologist and the following points were examined: the external surface, all orifices, the cranial cavity, the external surface of the brain and samples of the spinal cord, the thoracic and abdominal cavities and organs, the cervical tissues and organs, and the carcass. Cell masses from the injection site were fixed in 4% buffered formalin, dehydrated and embedded in a paraffin wax. Sections (5µm) were stained with hematoxylin / Eosin and analyzed by a pathologist for the presence of teratoma.

Biodistribution/toxicity GLP study

Nude rats (SPF (Specific Pathogen Free) Nude: Foxn1rnu) were purchased from Envigo and grafted at 7 weeks. Animals were fed ad libitum and exposed to an artificial day/light cycle of 12 hours. Males and females were treated with a hESC-RPE suspension (150000 cells), a hESC-RPE sheet (3.46mm^2) or a saline solution (3µl, Cooper) and sacrificed (after an overnight fasting) at week 2, week 13 and for the hESC-RPE

sheet an additional time point at week 26. Body weight and food consumption were evaluated during the study. A full detailed necropsy by an anatomopathologist was carried for all animals and organs/ tissues were sampled for the biodistribution analysis (see **supplementary table S4**). Biodistribution analysis was performed by a GLP laboratory (Genosafe, Evry, France). Briefly, human cells were detected in organ/tissue samples by quantitative real-time PCR on DNA extracts using a specific human *ALU* sequence. The qPCR method was validated to detect 1 human cell in 150,000-500,000 rat cells.

Statistical Analysis

GraphPad Prism 5 (GraphPad Software, Inc.) was used for statistical analysis. Significant ANOVAs were followed up with Tukey's multiple comparisons test; $*p < 0.05$, $**p < 0.01$, and $***p < 0.001$. When two groups unpaired were analyzed, Mann Whitney test was used. For the comparison of two groups paired, Wilcoxon matched-pairs signed rank test was used. When more than two groups, Krukal-Wallis non-parametric test was used. Data are expressed as mean +/- S.E.M, except if mentioned differently. Complete statistical analysis, containing detailed number of replicates, can be found in supplementary information.

Author contributions

SB performed monkey surgery, assisted with EB, CJ and KB. CMF and JD anesthetized primates, performed immunosuppression and were involved in primate housing. EB and CJ performed primate ophthalmic exams. KB performed stability assessment of the hESC-RPE sheet. CM and KB developed the medical devices. KB performed medical device experiments. SB, EB and KB conducted pig eye experiments. SB and EB developed the implantation strategy in monkeys. AP, WH and KB performed cell culture for rodent studies. MJ and WH prepared hAM scaffolds. KB and WH performed RPE quality control evaluations. KB performed rat eye surgeries and primate histology. JAS, MP, OG and CM provided resources. KB, JAS, MP, OG and CM designed the study and discussed the data. KB, OG and CM wrote the manuscript. All authors reviewed the manuscript.

Conflict of interest statement

KB, WH and CM are inventors of a pending patent related to the medical devices presented in this study. JAS and OG are inventors on patents (EP2989200 and WO2018149985) related to Methods for obtaining retinal progenitors, RPE cells and neural retinal cells from hPSCs. JAS is a consultant for Pixium Vision, GenSight Biologics, and Gene Signal and has personal financial interests in GenSight Biologics, Chronocam, ChronoLife, Pixium Vision, Tilak Healthcare, and SparingVision. All other authors declare that they have no competing interests.

Acknowledgments
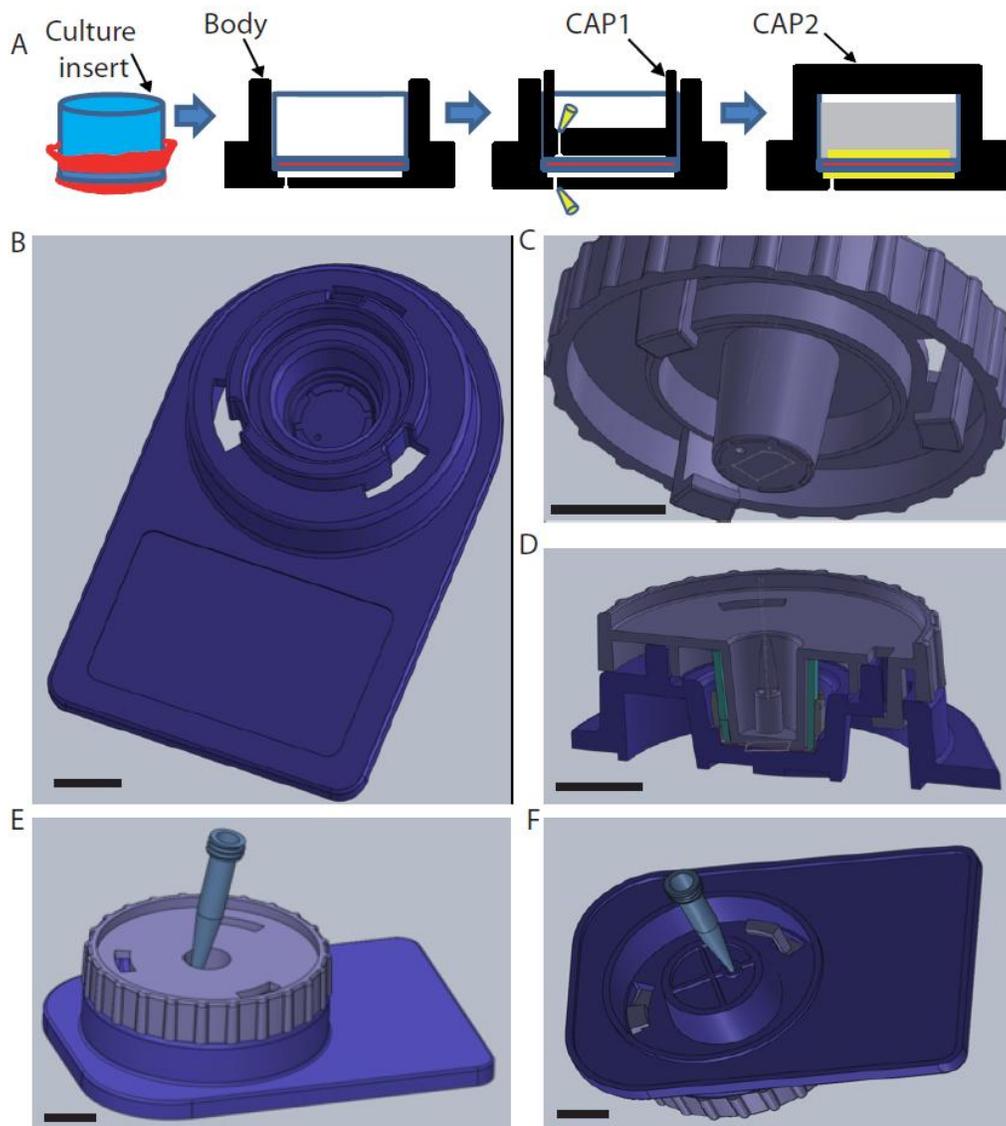
Figures and figure legends

Figure 1: Description of the medical device MD1 used to prepare the hESC-RPE sheet embedded in gelatin.

A. Scheme describing the sequential steps of hESC-RPE sheet embedded in gelatin into the medical device MD1. The hESC-RPE sheet (red) cultured in an insert (blue) is transferred to the MD1 body, then the MD1 body is closed with cap 1 and the gelatin (yellow) is added in both sides. The cap 1 is then removed, a transport media (grey) is added and the system is closed with a cap 2. **B,C.** Images of a MD1

central body and the cap 1. **D**. Transversal view of the MD1 body + cap 1. **E, F**. Positions of the tips to fill

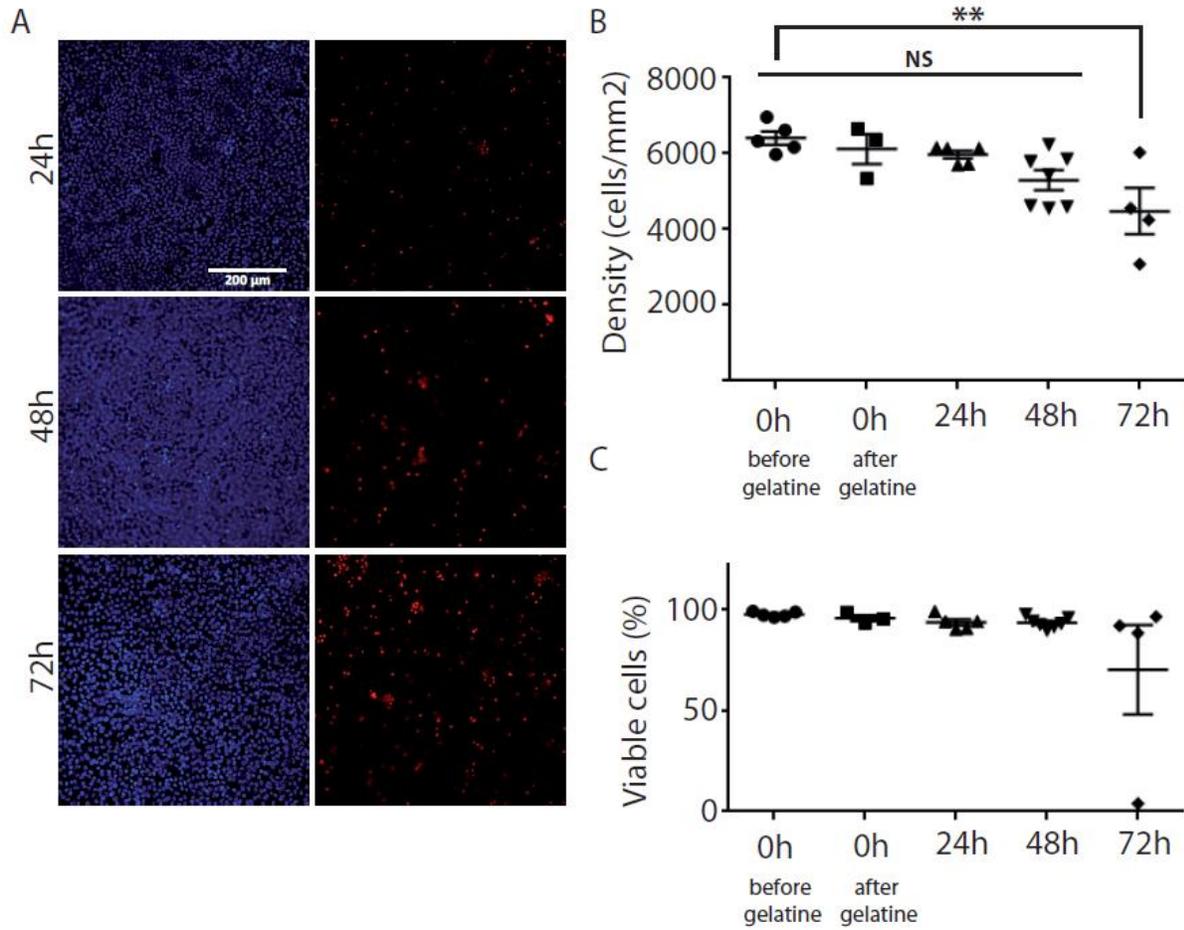the upper and lower side of the MD1. Scale bar = 1cm.

Figure 2: The hESC-RPE sheet embedded in gelatin is stable at 4°C for 48h.

A. Images of hESC-RPE sheet stained with Hoescht 33342 (total cell labelling, blue) and propidium iodide (dead cell labelling, red) after 24h, 48h and 72h of storage at 4°C in the MD1. **B.** Evaluation of the cell density at different time points before and after embedding in gelatin. **C.** Quantification of the number of live cells at different time points before and after embedding in gelatin. Data are expressed as mean +/- SEM. **p<0.01.
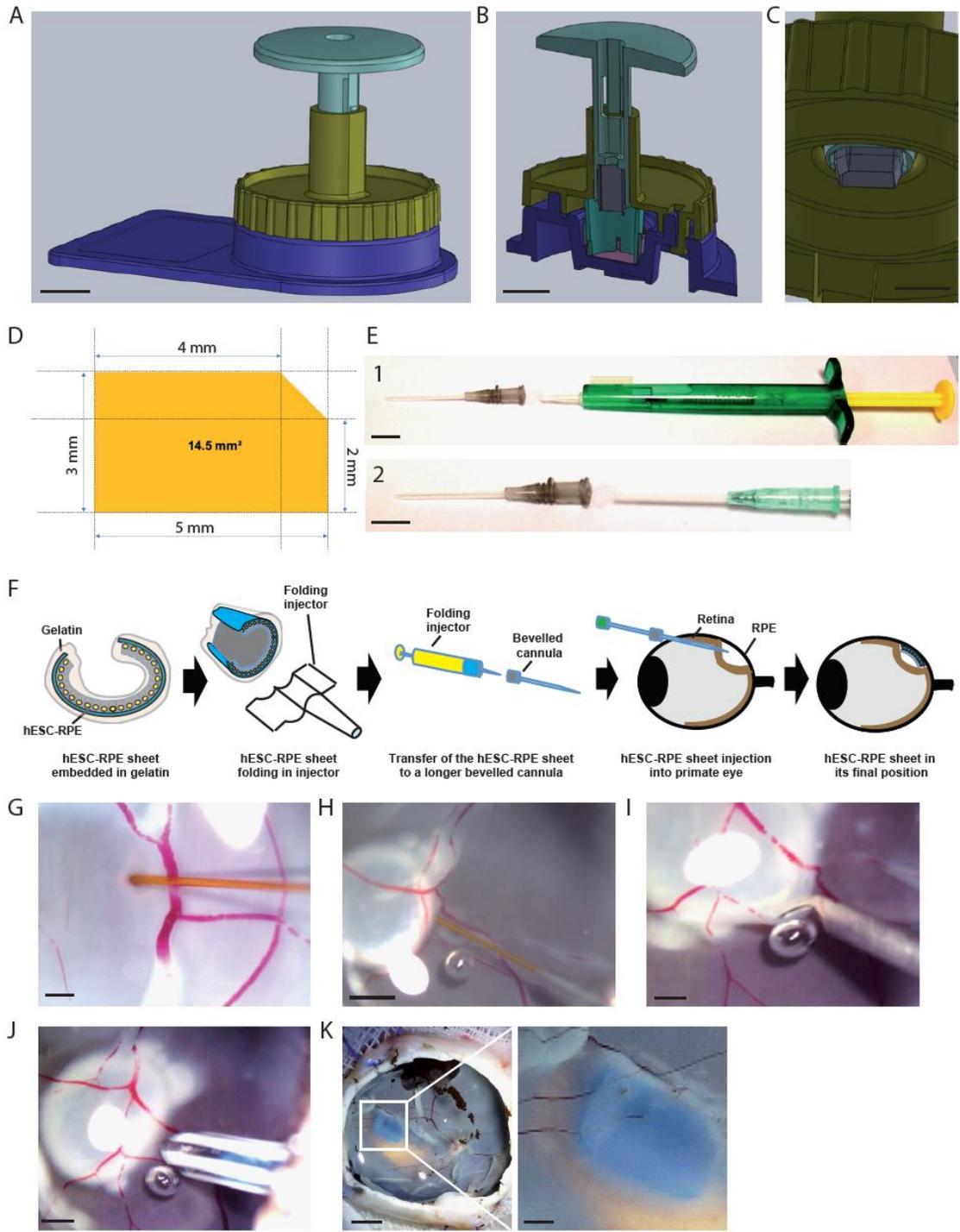
Figure 3: Description of the medical device MD2 used to prepare the hESC-RPE sheet and sheet implantation procedure in enucleated pig eyes.

A. Image showing the MD2 composed of the cap 3 (yellow) and the blade (green), fixed on the MD1 body (blue). Scale bar = 1cm. **B.** Transversal view of the MD2 mounted in the MD1. Scale bar = 1cm. **C.** Magnification showing the shape of the blade (SIM-card shape). Scale bar = 5mm. **D.** Size of the hESC-RPE sheet to be implanted. **E**. Transplantation tools to deliver the hESC-RPE sheet into the subretinal space. The system is composed of lens injector (green and yellow) were the hESC-RPE sheet is loaded and folded (panel 1). The hESC-RPE sheet is then transferred folded into a cannula (grey head) and the hESC-RPE sheet is then pushed into the eye with another cannula of lower size (light green; panel 2). Scale bar = 1cm. **F.** Scheme describing the loading of the hESC-RPE sheet into the injection system and grafting approach into large eyes. **G-J.** Sequential steps to transplant the hESC-RPE sheet in enucleated pig eyes: creation of a retinal detachment (G (Scale bar = 200µm), H (Scale bar = 1mm)); retinotomy (I (Scale bar = 200µm)) and delivery of the hESC-RPE sheet using the cannula (J (Scale bar = 1mm)) described in (E). **K**. Image showing the hESC-RPE sheet transplanted in an enucleated pig eye with a magnification of the graft on the right image. Scale bar = 5mm and 1mm for the magnification.
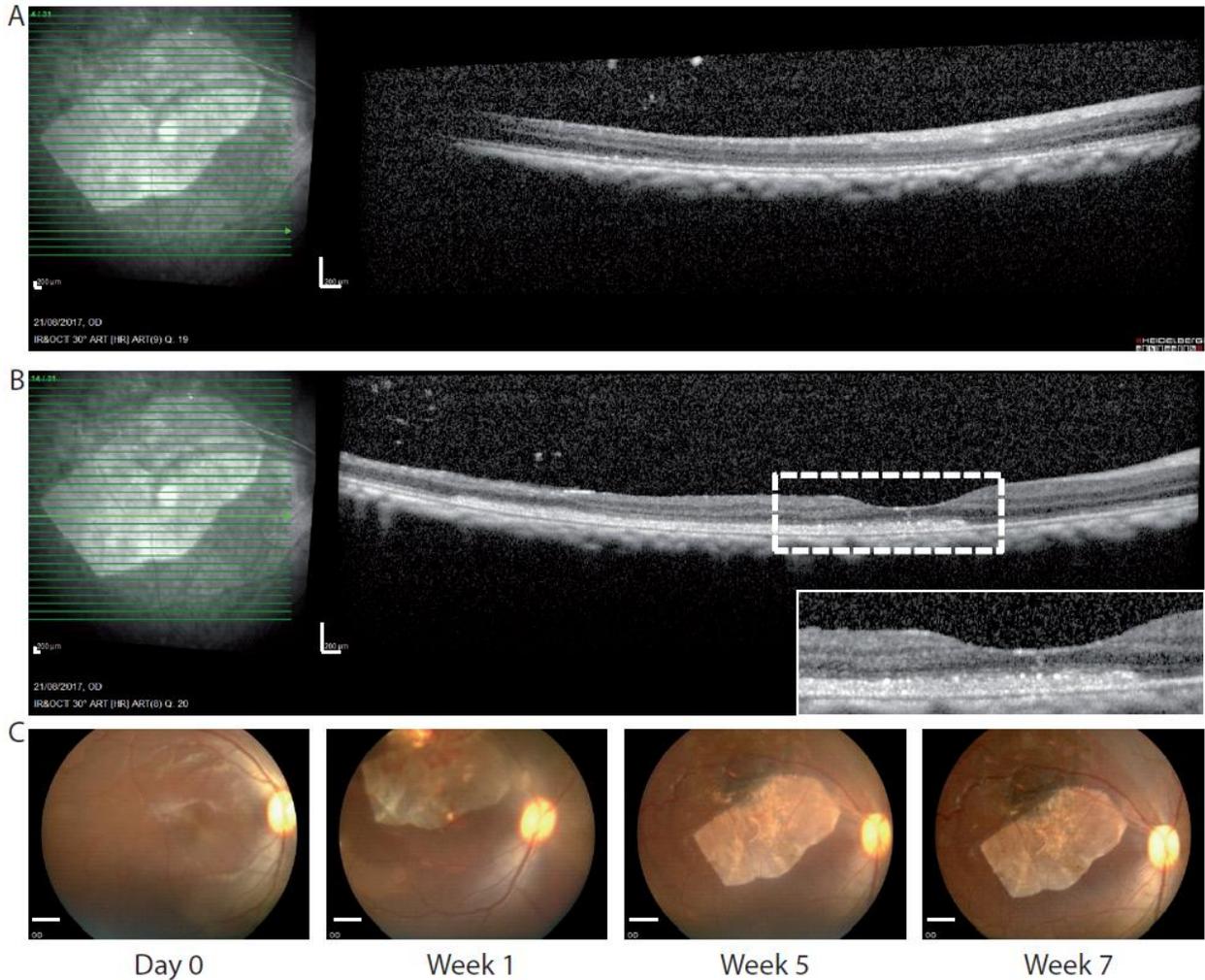
Figure 4: The hESC-RPE sheet is grafted under the macular area in nonhuman primates and keep its initial position during the experimental period.

A. Optical coherence section of a nonhuman primate transplanted with the hESC-RPE sheet in an area distant to the graft. The position of the section is indicated on the left image with a bold green arrow. Scale bar = 200µm. **B**. Optical coherence section of a nonhuman primate transplanted with the hESC-RPE sheet in the foveal area. The position of the section is indicated on the left image with a bold green arrow. The graft is localized under the fovea (magnification of the white box on the lower right image). **C.**

Eye fundus images of the same animal at different time points before and after the surgery. The hESC-

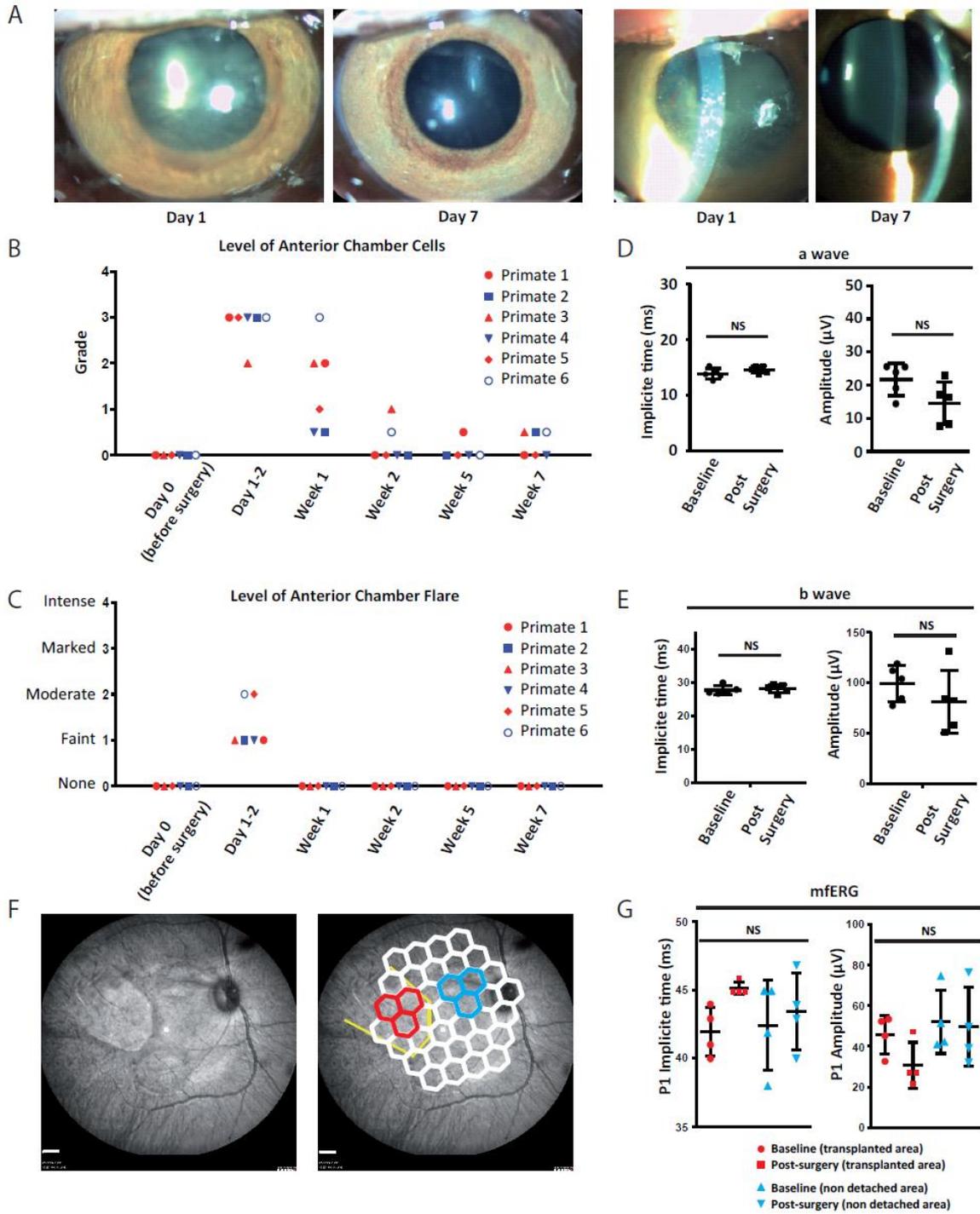RPE sheet remains at the same position during the follow up. Scale bar = 1mm.

Figure 5: No alteration of the retinal function following hESC-RPE sheet implantation in nonhuman primates.

A. Slit lamp biomicroscopy images of the same eye the day after the surgery and one week after the surgery. **B-C.** Quantification of the level of anterior chamber cells (B) and anterior chamber flare (C) at different time points before and after surgery. A transitory inflammation is observed just after the surgery that resolves at week 2. Each primate is represented individually. **D-E**. Full field photopic electroretinography of each operated eye before and after the surgery showing implicit time and amplitude of the a wave (D) and b wave (E). Each primate is represented individually. **F.** Images of eye fundus showing the hESC-RPE sheet (left) and illustrating the different hexagons that are quantified at the graft position (in red) and near the graft (in blue), by Multifocal ERG (right). Scale bar = 1mm. **G.** Quantification of the P1 implicit time (left graph) and the P1 amplitude (right graph) obtained by mfERG. Each primate is represented independently.
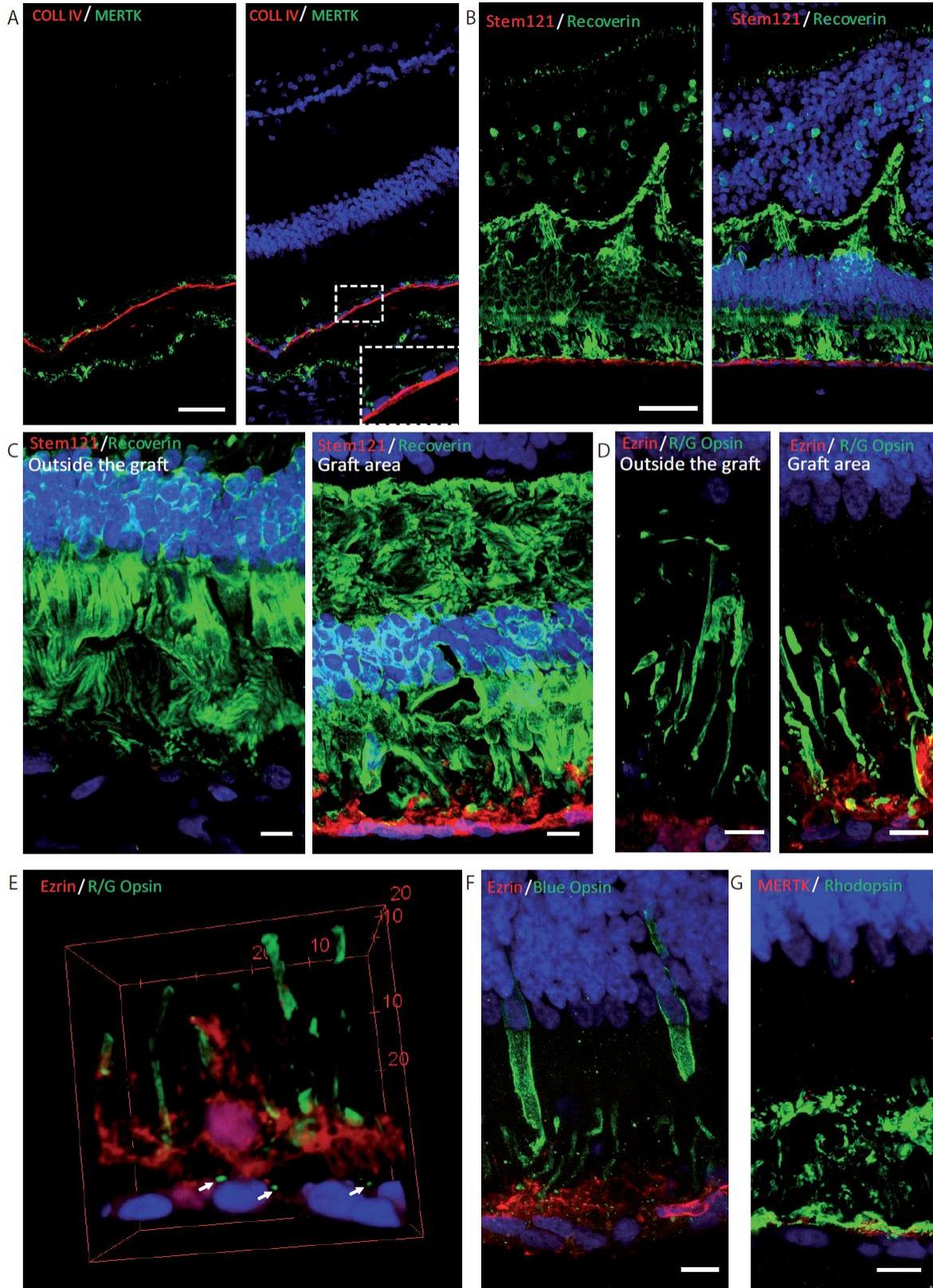
Figure 6: Survival of hESC-RPE sheets grafted in nonhuman primate eye in close contact with host photoreceptors.

A. Immunofluorescence on nonhuman primate retinal section with antibodies against Collagen IV (human specific marker, red) and MERTK (green) allowed the identification of respectively amniotic membrane and RPE cells. Nuclei are counterstained with DAPI (blue). Scale bar =50μm. B. Maximal projection of a stack of images of a monkey retina transplanted with a hESC-RPE sheet. The human specific marker Stem121 (in red) identifies grafted human cells that are in contact with host photoreceptors expressing Recoverin (in green). Nuclei are counterstained with DAPI. Scale bar =50μm. C. Comparison of the expression of Recoverin (in green) in the graft area and outside the transplant area. Stem121 (in red) identifies grafted human cells. Nuclei are counterstained with DAPI. Scale bar =10μm. D. Immunofluorescence on retinal sections of a nonhuman primate eye in the graft area and outside the transplant are. Cones are detected with antibodies targeting Red/Green opsin (green) and the apical side of hESC-RPE is identified with Ezrin (red). Nuclei are counterstained with DAPI. Scale bar =10μm. E. 3D reconstruction of retinal section immunostained with antibodies against Ezrin (red) and Red/Green opsin (green). White arrows indicate phagocytosis events. For the 3 axes, units are in μm. F-G. Immunofluorescence on nonhuman primate retinal section with antibodies against Ezrin (red) and Blue opsin (green) (F) and against MERTK (red) and Rhodopsin (green) (G). Nuclei are counterstained with DAPI. Scale bar =10μm.
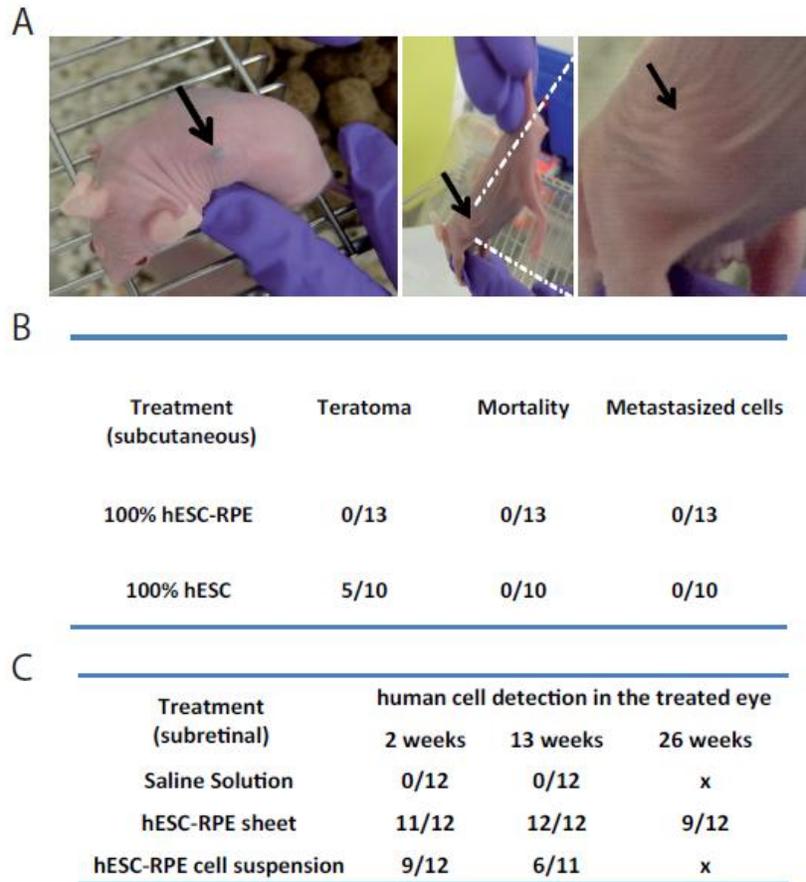
Figure 7: hESC-RPE cells or sheets are safe in rodents.

A. Images of Nude mice transplanted with hESC-RPE cell suspension (left image) or hESCs (middle and right images) through a subcutaneous route. Black arrows indicate the location of the cell mass close to the injection site. B. Table recapitulating the results of the teratoma study conducted in Nude mice. hESC-RPE grafting resulted in no teratoma formation, mortality or metastasized cells in other organs. C. Table recapitulation the results of the biodistribution study (in the treated eye) in Nude rats grafted in the subretinal space with hESC-RPE sheets, hESC-RPE cell suspension or a control saline solution. hESC-RPE sheets survived better in the eye compared to cell suspensions.

Data availability

The two medical devices presented in this study are available upon request.

References

1.   Strauss O. The retinal pigment epithelium in visual function. *Physiological reviews.*
        2005;85(3):845-81.
2.   Berger W, Kloeckener-Gruissem B, and Neidhardt J. The molecular basis of human retinal and
        vitreoretinal diseases. *Progress in retinal and eye research.* 2010;29(5):335-75.
3.   Verbakel SK, van Huet RAC, Boon CJF, den Hollander AI, Collin RWJ, Klaver CCW, Hoyng CB,
        Roepman R, and Klevering BJ. Non-syndromic retinitis pigmentosa. *Progress in retinal and eye
        research.* 2018;66(157-86.
4.   Gagliardi G, Ben M'Barek K, and Goureau O. Photoreceptor cell replacement in macular
        degeneration and retinitis pigmentosa: A pluripotent stem cell-based approach. *Progress in
        retinal and eye research.* 2019.
5.   Ben M'Barek K, and Monville C. Cell Therapy for Retinal Dystrophies: From Cell Suspension
        Formulation to Complex Retinal Tissue Bioengineering. *Stem cells international.*
        2019;2019(4568979.
6.   Russell S, Bennett J, Wellman JA, Chung DC, Yu ZF, Tillman A, Wittes J, Pappas J, Elci O, McCague
        S, et al. Efficacy and safety of voretigene neparvovec (AAV2-hRPE65v2) in patients with RPE65-
        mediated inherited retinal dystrophy: a randomised, controlled, open-label, phase 3 trial. *Lancet.*
        2017;390(10097):849-60.
7.   Khandhadia S, Cherry J, and Lotery AJ. Age-related macular degeneration. *Advances in
        experimental medicine and biology.* 2012;724(15-36.
8.   Ferris FL, 3rd, Wilkinson CP, Bird A, Chakravarthy U, Chew E, Csaky K, Sadda SR, and Beckman
        Initiative for Macular Research Classification C. Clinical classification of age-related macular
        degeneration. *Ophthalmology.* 2013;120(4):844-51.
9.   Guillonneau X, Eandi CM, Paques M, Sahel JA, Sapieha P, and Sennlaub F. On phagocytes and
        macular degeneration. *Progress in retinal and eye research.* 2017;61(98-128.
10.   Fritsche LG, Chen W, Schu M, Yaspan BL, Yu Y, Thorleifsson G, Zack DJ, Arakawa S, Cipriani V,
        Ripke S, et al. Seven new loci associated with age-related macular degeneration. *Nature genetics.*
        2013;45(4):433-9, 9e1-2.
11.   Mitchell P, Liew G, Gopinath B, and Wong TY. Age-related macular degeneration. *Lancet.*
        2018;392(10153):1147-59.
12.   Binder S, Stanzel BV, Krebs I, and Glittenberg C. Transplantation of the RPE in AMD. *Progress in
        retinal and eye research.* 2007;26(5):516-54.
13.   Kashani AH, Lebkowski JS, Rahhal FM, Avery RL, Salehi-Had H, Dang W, Lin CM, Mitra D, Zhu D,
        Thomas BB, et al. A bioengineered retinal pigment epithelial monolayer for advanced, dry age-
        related macular degeneration. *Sci Transl Med.* 2018;10(435).
14.   Schwartz SD, Hubschman JP, Heilwell G, Franco-Cardenas V, Pan CK, Ostrick RM, Mickunas E, Gay
        R, Klimanskaya I, and Lanza R. Embryonic stem cell trials for macular degeneration: a preliminary
        report. *Lancet.* 2012;379(9817):713-20.

15. Schwartz SD, Regillo CD, Lam BL, Eliott D, Rosenfeld PJ, Gregori NZ, Hubschman JP, Davis JL, Heilwell G, Spirn M, et al. Human embryonic stem cell-derived retinal pigment epithelium in patients with age-related macular degeneration and Stargardt's macular dystrophy: follow-up of two open-label phase 1/2 studies. *Lancet.* 2015;385(9967):509-16.

16. da Cruz L, Fynes K, Georgiadis O, Kerby J, Luo YH, Ahmado A, Vernon A, Daniels JT, Nommiste B, Hasan SM, et al. Phase 1 clinical study of an embryonic stem cell-derived retinal pigment epithelium patch in age-related macular degeneration. *Nature biotechnology.* 2018;36(4):328-37.

17. Mandai M, Watanabe A, Kurimoto Y, Hirami Y, Morinaga C, Daimon T, Fujihara M, Akimaru H, Sakai N, Shibata Y, et al. Autologous Induced Stem-Cell-Derived Retinal Cells for Macular Degeneration. *The New England journal of medicine.* 2017;376(11):1038-46.

18. Roska B, and Sahel JA. Restoring vision. *Nature.* 2018;557(7705):359-67.

19. Nazari H, Zhang L, Zhu D, Chader GJ, Falabella P, Stefanini F, Rowland T, Clegg DO, Kashani AH, Hinton DR, et al. Stem cell based therapies for age-related macular degeneration: The promises and the challenges. *Progress in retinal and eye research.* 2015;48(1-39.

20. Zarbin M, Sugino I, and Townes-Anderson E. Concise Review: Update on Retinal Pigment Epithelium Transplantation for Age-Related Macular Degeneration. *Stem cells translational medicine.* 2019.

21. Diniz B, Thomas P, Thomas B, Ribeiro R, Hu Y, Brant R, Ahuja A, Zhu D, Liu L, Koss M, et al. Subretinal implantation of retinal pigment epithelial cells derived from human embryonic stem cells: improved survival when implanted as a monolayer. *Investigative ophthalmology & visual science.* 2013;54(7):5087-96.

22. Ben M'Barek K, Habeler W, Plancheron A, Jarraya M, Regent F, Terray A, Yang Y, Chatrousse L, Domingues S, Masson Y, et al. Human ESC-derived retinal epithelial cell sheets potentiate rescue of photoreceptor cell loss in rats with retinal degeneration. *Sci Transl Med.* 2017;9(421).

23. Sharma R, Khristov V, Rising A, Jha BS, Dejene R, Hotaling N, Li Y, Stoddard J, Stankewicz C, Wan Q, et al. Clinical-grade stem cell-derived retinal pigment epithelium patch rescues retinal degeneration in rodents and pigs. *Science translational medicine.* 2019;11(475).

24. Paolin A, Cogliati E, Trojan D, Griffoni C, Grassetto A, Elbadawy HM, and Ponzin D. Amniotic membranes in ophthalmology: long term data on transplantation outcomes. *Cell and tissue banking.* 2016;17(1):51-8.

25. Kiilgaard JF, Scherfig E, Prause JU, and la Cour M. Transplantation of amniotic membrane to the subretinal space in pigs. *Stem cells international.* 2012;2012(716968.

26. He H, Tan Y, Duffort S, Perez VL, and Tseng SC. In vivo downregulation of innate and adaptive immune responses in corneal allograft rejection by HC-HA/PTX3 complex purified from amniotic membrane. *Investigative ophthalmology & visual science.* 2014;55(3):1647-56.

27. Ben M'Barek K, Habeler W, Plancheron A, Jarraya M, Goureau O, and Monville C. Engineering Transplantation-suitable Retinal Pigment Epithelium Tissue Derived from Human Embryonic Stem Cells. *Journal of visualized experiments : JoVE.* 2018139).

28. Kanemura H, Go MJ, Shikamura M, Nishishita N, Sakai N, Kamao H, Mandai M, Morinaga C, Takahashi M, and Kawamata S. Tumorigenicity studies of induced pluripotent stem cell (iPSC)-derived retinal pigment epithelium (RPE) for the treatment of age-related macular degeneration. *PloS one.* 2014;9(1):e85336.

29. Kawamata S, Kanemura H, Sakai N, Takahashi M, and Go MJ. Design of a Tumorigenicity Test for Induced Pluripotent Stem Cell (iPSC)-Derived Cell Products. *Journal of clinical medicine.* 2015;4(1):159-71.

30.   Kamao H, Mandai M, Okamoto S, Sakai N, Suga A, Sugita S, Kiryu J, and Takahashi M. Characterization of human induced pluripotent stem cell-derived retinal pigment epithelium cell sheets aiming for clinical application. *Stem cell reports.* 2014;2(2):205-18.

31.   Lund RD, Wang S, Klimanskaya I, Holmes T, Ramos-Kelsey R, Lu B, Girman S, Bischoff N, Sauve Y, and Lanza R. Human embryonic stem cell-derived cells rescue visual function in dystrophic RCS rats. *Cloning and stem cells.* 2006;8(3):189-99.

32.   Idelson M, Alper R, Obolensky A, Ben-Shushan E, Hemo I, Yachimovich-Cohen N, Khaner H, Smith Y, Wiser O, Gropp M, et al. Directed differentiation of human embryonic stem cells into functional retinal pigment epithelium cells. *Cell stem cell.* 2009;5(4):396-408.

33.   Lu B, Malcuit C, Wang S, Girman S, Francis P, Lemieux L, Lanza R, and Lund R. Long-term safety and function of RPE from human embryonic stem cells in preclinical models of macular degeneration. *Stem cells.* 2009;27(9):2126-35.

34.   Tezel TH, Del Priore LV, and Kaplan HJ. Reengineering of aged Bruch's membrane to enhance retinal pigment epithelium repopulation. *Investigative ophthalmology & visual science.* 2004;45(9):3337-48.

35.   Stanzel BV, Liu Z, Somboonthanakij S, Wongsawad W, Brinken R, Eter N, Corneo B, Holz FG, Temple S, Stern JH, et al. Human RPE stem cells grown into polarized RPE monolayers on a polyester matrix are maintained after grafting into rabbit subretinal space. *Stem cell reports.* 2014;2(1):64-77.

36.   Hsiung J, Zhu D, and Hinton DR. Polarized human embryonic stem cell-derived retinal pigment epithelial cell monolayers have higher resistance to oxidative stress-induced cell death than nonpolarized cultures. *Stem cells translational medicine.* 2015;4(1):10-20.

37.   Sonoda S, Sreekumar PG, Kase S, Spee C, Ryan SJ, Kannan R, and Hinton DR. Attainment of polarity promotes growth factor secretion by retinal pigment epithelial cells: relevance to age-related macular degeneration. *Aging.* 2009;2(1):28-42.

38.   Ben M'Barek K, Habeler W, and Monville C. Stem Cell-Based RPE Therapy for Retinal Diseases: Engineering 3D Tissues Amenable for Regenerative Medicine. *Advances in experimental medicine and biology.* 2018;1074(625-32.

39.   Jin ZB, Gao ML, Deng WL, Wu KC, Sugita S, Mandai M, and Takahashi M. Stemming retinal regeneration with pluripotent stem cells. *Progress in retinal and eye research.* 2018.

40.   Bendali A, Rousseau L, Lissorgues G, Scorsone E, Djilas M, Degardin J, Dubus E, Fouquet S, Benosman R, Bergonzo P, et al. Synthetic 3D diamond-based electrodes for flexible retinal neuroprostheses: Model, production and in vivo biocompatibility. *Biomaterials.* 2015;67(73-83.

41.   Lorach H, Lei X, Galambos L, Kamins T, Mathieson K, Dalal R, Huie P, Harris J, and Palanker D. Interactions of Prosthetic and Natural Vision in Animals With Local Retinal Degeneration. *Investigative ophthalmology & visual science.* 2015;56(12):7444-50.

42.   Andrews PW, Baker D, Benvinisty N, Miranda B, Bruce K, Brustle O, Choi M, Choi YM, Crook JM, de Sousa PA, et al. Points to consider in the development of seed stocks of pluripotent stem cells for clinical applications: International Stem Cell Banking Initiative (ISCBI). *Regenerative medicine.* 2015;10(2 Suppl):1-44.

43.   Taylor CJ, Bolton EM, Pocock S, Sharples LD, Pedersen RA, and Bradley JA. Banking on human embryonic stem cells: estimating the number of donor cell lines needed for HLA matching. *Lancet.* 2005;366(9502):2019-25.

44.   Wilmut I, Leslie S, Martin NG, Peschanski M, Rao M, Trounson A, Turner D, Turner ML, Yamanaka S, and Taylor CJ. Development of a global network of induced pluripotent stem cell haplobanks. *Regenerative medicine.* 2015;10(3):235-8.

45.   Taylor CJ, Peacock S, Chaudhry AN, Bradley JA, and Bolton EM. Generating an iPSC bank for HLA-matched tissue transplantation based on known donor and recipient HLA types. *Cell stem cell.* 2012;11(2):147-52.

46.   De Sousa PA, Tye BJ, Bruce K, Dand P, Russell G, Collins DM, Greenshields A, McDonald K, Bradburn H, Canham MA, et al. Derivation of the clinical grade human embryonic stem cell line RCe013-A (RC-9). *Stem cell research.* 2016;17(1):36-41.